Redox Biology 60 (2023) 102599

Contents lists available at ScienceDirect

Redox Biology

journal homepage: www.elsevier.com/locate/redox

Avasopasem manganese (GC4419) protects against cisplatin-induced chronic kidney disease: An exploratory analysis of renal metrics from a randomized phase 2b clinical trial in head and neck cancer patients

K.A. Mapuskar [a], G. Vasquez Martinez [b], C.F. Pulliam [a], M.S. Petronek [a], E.J. Steinbach [c], V. Monga [d], M. Furqan [d], J.G. Jetton [e], D.P. Saunders [f], A. Pearce [f], S. Davidson [f], L. Pitre [f], N.E. Dunlap [g], R. Fairbanks [h], C.M. Lee [h], S.L. Mott [i], K.L. Bodeker [a], Huang Cl [j], J.M. Buatti [a], C.M. Anderson [a], R.A. Beardsley [k], J.T. Holmlund [k], D. Zepeda-Orozco [b,l], D.R. Spitz [a,*], B.G. Allen [a,**]

[a] University of Iowa Hospitals and Clinics, Free Radical and Radiation Biology Program, Department of Radiation Oncology, Iowa City, IA, USA
[b] Kidney and Urinary Tract Center, The Abigail Wexner Research Institute at Nationwide Children's Hospital, Columbus, OH, USA
[c] The University of Iowa Stead Family Department of Pediatrics, Iowa City, IA, USA
[d] University of Iowa Hospitals and Clinics, Department of Internal Medicine, Iowa City, IA, USA
[e] Medical College of Wisconsin, Department of Pediatrics, Milwaukee, WI, USA
[f] Northeast Cancer Centre, Health Sciences North, Northern Ontario School of Medicine, Sudbury, Canada
[g] University of Louisville, School of Medicine, Louisville, KY, 40202, USA
[h] Cancer Care Northwest, Spokane, WA, USA
[i] University of Iowa Holden Comprehensive Cancer Center, Iowa City, IA, USA
[j] University of Iowa Carver College of Medicine, Department of Internal Medicine, Iowa City, IA, USA
[k] Galera Therapeutics, Inc., Malvern, PA, USA
[l] Department of Pediatrics, The Ohio State University College of Medicine, Columbus, OH, USA

ARTICLE INFO

Keywords:
Superoxide dismutase mimetic
Avasopasem manganese
GC4419
Cisplatin
Radiation
Kidney injury
eGFR
Acute kidney disease
Chronic kidney disease
Epithelial growth factor
Iron

ABSTRACT

Head and neck squamous cell carcinoma (HNSCC) patients treated with high-dose cisplatin concurrently with radiotherapy (hdCis-RT) commonly suffer kidney injury leading to acute and chronic kidney disease (AKD and CKD, respectively). We conducted a retrospective analysis of renal function and kidney injury-related plasma biomarkers in a subset of HNSCC subjects receiving hdCis-RT in a double-blinded, placebo-controlled clinical trial (NCT02508389) evaluating the superoxide dismutase mimetic, avasopasem manganese (AVA), an investigational new drug. We found that 90 mg AVA treatment prevented a significant reduction in estimated glomerular filtration rate (eGFR) three months as well as six and twelve months after treatment compared to 30 mg AVA and placebo. Moreover, AVA treatment may have allowed renal repair in the first 22 days following cisplatin treatment as evidenced by an increase in epithelial growth factor (EGF), known to aid in renal recovery. An upward trend was also observed in plasma iron homeostasis proteins including total iron (Fe-blood) and iron saturation (Fe-saturation) in the 90 mg AVA group versus placebo. These data support the hypothesis that treatment with 90 mg AVA mitigates cisplatin-induced CKD by inhibiting hdCis-induced renal changes and promoting renal recovery.

1. Introduction

High-dose cisplatin (100 mg/m^2, once every three weeks)

* Corresponding author. Division of Free Radical and Radiation Biology Department of Radiation Oncology The University of Iowa Hospitals and Clinics, Iowa City, IA, 52242, USA.
** Corresponding author. Division of Free Radical and Radiation Biology Department of Radiation Oncology The University of Iowa Hospitals and Clinics, Iowa City, IA, 52242-1181, USA.
E-mail addresses: douglas-spitz@uiowa.edu (D.R. Spitz), bryan-allen@uiowa.edu (B.G. Allen).

https://doi.org/10.1016/j.redox.2022.102599
Received 16 December 2022; Received in revised form 29 December 2022; Accepted 30 December 2022
Available online 3 January 2023

administered concurrently with ionizing radiation therapy (RT, 60–70 Gy total in 2–2.2 Gy fractions) is a commonly used treatment regimen (hdCis-RT) for head and neck cancers (HNC) [1]. This regimen, however, is associated with significant toxicities, including acute and chronic nephrotoxicity [2].

Approximately 31–68% of patients treated with hdCis will experience acute cisplatin-induced nephrotoxicity within one week of cisplatin administration and an estimated 30% will go on to develop chronic kidney disease (CKD) long-term [3,4]. Recently, several studies identified acute kidney injury (AKI) and CKD as related parts of the same pathophysiological process of renal injury wherein patients with AKI have an increased risk of developing CKD which is worsened by other underlying risk factors including diabetes and advanced age [5,6]. However, cisplatin-induced AKI may be under-recognized based on the current serum creatinine definition. The most common presentation of kidney injury is tubular electrolyte wasting that results in hypokalemia, hypomagnesemia, and hypophosphatemia in up to 70% of patients compared to the incidence of 30% AKI predicted based on serum creatinine [7,8]. Markers of tubulointerstitial injury in AKI can predict the duration and recovery from AKI, as well as the development of CKD in human studies [9]. Based on these findings, a recent AKI consensus report recommends that biomarkers of tubulointerstitial disease be incorporated into post-AKI and AKD care to refine AKD staging and predict patient outcomes [9]. Thus, markers of tubulointerstitial disease may be useful to identify early the potential beneficial effects of renal protective therapies to prevent CKD [7,10].

hdCis-induced AKD and CKD are suggested to involve the production of superoxide ($O_2^{\bullet-}$) in the pathogenesis of initiation and transition from AKI to CKD in preclinical models [2,11,12]. Increased $O_2^{\bullet-}$ levels can cause reactive oxygen species (ROS)-mediated damage to normal tissues and thus result in tubular epithelial cell impairment [12-15]. $O_2^{\bullet-}$ is normally scavenged in cells by superoxide dismutases (SODs). Redox-active iron is another critical regulator of ROS damage, with the iron-binding protein, ferritin, responsible for preserving cellular iron homeostasis. Increased levels of ferritin may alleviate oxidative stress by the sequestration of free iron, impeding its role in Fenton reactions that generate ROS including hydroxyl radical [16-19].

The SOD mimetic, avasopasem manganese (AVA), selectively catalyzes the dismutation of $O_2^{\bullet-}$ to hydrogen peroxide (H_2O_2) which is then converted to water and oxygen by enzymes including catalase, glutathione peroxidases, and peroxiredoxins [20,21]. Preclinical work strongly suggested a role for AVA in reducing cisplatin-induced AKI and AKD [12]. Given these exciting data, it seemed opportune to investigate the effects of AVA on renal outcomes in a subset of subjects who received hdCis-RT in a randomized, double-blinded, placebo-controlled phase 2b trial, undertaken to evaluate the effect of AVA on severe oral mucositis.

Abbreviations:

(SOD) Superoxide Dismutase
(AVA or GC4419) Avasopasem Manganese
(hdCis) High Dose Cisplatin
(RT) Radiation Therapy
(hdCis-RT) High Dose Cisplatin concurrently with Radiation Therapy
(IMRT) Intensity-Modulated Radiotherapy
(HNC) Head and Neck Cancer
(HNSCC) Head and neck Squamous Cell Carcinoma
(SOM) Severe Oral Mucositis
(eGFR) Estimated Glomerular Filtration Rate
(AKI) Acute Kidney Injury
(AKD) Acute Kidney Disease
(CKD) Chronic Kidney Disease
(ROS) Reactive Oxygen Species
($O_2^{\bullet-}$) Superoxide
(H_2O_2) Hydrogen Peroxide
(NGAL) Neutrophil Gelatinase-Associated Lipocalin
(KIM-1) Kidney Injury Molecule-1
(TNFR1 and TNFR2) Tumor Necrosis Factor Receptors
(EGF) Epithelial Growth Factor
(4-Hydroxynonenal)-modified proteins 4HNE
(3NT) 3-Nitrotyrosine
(Fe-blood) Ferritin
(Fe-Saturation) Ferritin saturation
(Tf) Transferrin
(TIBC) and Total Iron Binding Capacity

2. Methods

2.1. Subjects

Subjects included in this analysis had pathologically confirmed squamous cell carcinoma of the oral cavity or oropharynx and received high-dose cisplatin (hdCis; 100 mg/m^2 every three weeks) plus concurrent intensity-modulated radiotherapy (IMRT) delivered as single daily fractions of 2.0–2.2 Gy reaching a cumulative dose of 60–70 Gy. These subjects had participated at the University of Iowa in an industry-sponsored (Galera Therapeutics), randomized, double-blind, placebo-controlled, multicenter trial (NCT02508389) of avasopasem to reduce severe oral mucositis (SOM), the primary results of which have been published [22], Subjects participating in NCT02508389 were randomly assigned to one of three treatment arms: placebo (bicarbonate-buffered 0.9% saline), or 30 mg or 90 mg AVA (in the same vehicle), each given daily within 1 h prior to IMRT as a 60 min IV infusion. As part of the study, these subjects were followed for oncologic outcomes every 3 months after treatment for the first year and every 4 months for the second year. All subjects received intravenous hydration as part of the institutional standard of care.

Table 1 summarizes the characteristics of the randomized trial subjects included in the present report. This is a post-hoc selected subset from the randomized trial which included a total of 88 subjects receiving hdCis: 31 receiving avasopasem 90 mg, 29 receiving avasopasem 30 mg, and 28 receiving Placebo. Selection was based solely on the availability of the necessary renal follow-up data and appropriate subject consent.

2.2. Ethics and oversight

The IRB of record for the parent clinical trial (GT-201, NCT02508389) was the University of Iowa Biomedical IRB (IRB00000099, FWA000003007). Prospective consent for future use of blood specimens was obtained from all participants; this was optional with the allowance to have samples destroyed at a future date if desired. Research use of these codified specimens was considered exempt under 45 CFR 46.104(d) [4](ii). Good Clinical Practice as defined by ICH E6 (R2) and as adopted by U.S. Federal Law was applied to both the parent study and secondary specimen analysis.

2.3. Assessment of renal outcomes

Kidney function markers including serum blood urea nitrogen (BUN)

Table 1
Baseline Patient Characteristics and Treatment Delivery Details. Fisher's exact tests were used to compare categorical variables, and t-tests were used to compare continuous variables between treatment groups. Abbreviations: N, Number of Subjects; Col %, Column Percent.

Covariate	Statistics	Level	Treatment Group			P-value
			Placebo	30 mg	90 mg	
			N = 8	N = 7	N = 9	
Gender	N (Col %)	Female	0 (0)	1 (14.3)	1 (11.1)	0.74
	N (Col %)	Male	8 (100)	6 (85.7)	8 (88.9)	
Race	N (Col %)	Black	0 (0)	1 (14.3)	0 (0)	0.29
	N (Col %)	White	8 (100)	6 (85.7)	9 (100)	
Ethnicity	N (Col %)	Non-Hispanic	8 (100)	7 (100)	9 (100)	–
Current Tobacco Use	N (Col %)	No	8 (100)	6 (85.7)	6 (66.7)	0.27
	N (Col %)	Yes	0 (0)	1 (14.3)	3 (33.3)	
Current Alcohol Use	N (Col %)	No	4 (50.0)	5 (71.4)	3 (33.3)	0.36
	N (Col %)	Yes	4 (50.0)	2 (28.6)	6 (66.7)	
Age	Median		56	58	54	0.16
	Range		(49–64)	(56–64)	(42–65)	
BUN (mg/dL)	Median		13	13	10	0.50
	Range		[9-16]	[7-22]	[6-22]	
Creatinine (mg/dL)	Median		0.8	0.9	0.8	0.20
	Range		(0.6–1.0)	(0.8–1.1)	(0.6–1.1)	
eGFR (mL/min/1.73m2)	Median		90	85	90	0.18
	Range		(77–90)	(69–90)	(71–90)	
Treatment Duration (weeks)	Median		7.0	7.0	7.0	1.00
	Range		(6.4–7.9)	(6.3–7.4)	(6.3–7.3)	
Cumulative Cisplatin Dose (mg/m^2) (	Median		300	300	300	0.65
	Range		(175–300)	(175–300)	(175–300)	

and creatinine (Cr) were obtained from electronic medical records pre-hdCis-RT (**D0**), 3 weeks (**D22**, prior to second cisplatin dose) and 6 weeks (**D43,** prior to third cisplatin dose), and 3 months (**M3**), 6 months (**M6**) and 12 months (**M12**) after completion of to assess longitudinal changes within each treatment group (Illustration 1**)**. The estimated glomerular filtration rate (eGFR) was derived from the Chronic Kidney Disease Epidemiology (CKD-EPI) creatinine-based equation at the same time points.

Additional exploratory kidney injury biomarkers were evaluated pre-hdCis-RT on (**D0**) and on (**D22**) since serum samples were collected only at these time points. Evaluation of tubulointerstitial disease biomarkers were performed on U-Plex plates by electrochemiluminescence using the MESO QuickPlex SQ 120 instrument [Meso Scale Discovery (MSD) Platform, Rockville, MD, USA] according to manufacturer's instructions. Analysis of these was performed using the Discovery Workbench 4.0 Analysis Software. Standard curves for each analyte were measured and plotted to calculate the concentration of each sample. Exploratory biomarkers measured using the MSD platform included Neutrophil Gelatinase-Associated Lipocalin (NGAL), Kidney Injury Molecule-1 (KIM-1), Cystatin C, Tumor Necrosis Factor Receptors (TNFR1 and TNFR2), Epithelial Growth Factor (EGF), Osteopontin, Osteoactivin, and Uromodulin.

Serum BUN (10–20 mg/dL, any gender) and creatinine (Males: 0.6–1.2 mg/dL, Females: 0.5–1.0 mg/dL) levels were evaluated using the reference ranges defined by Emory Warner Pathology Laboratories (CLIA 16D0664625) at the University of Iowa. eGFR was derived from the Chronic Kidney Disease Epidemiology (CKD-EPI) formula and staged as defined by Kidney Disease Improving Global Outcomes (KDIGO) guidelines [23].

Kidney disease was assessed using the KDIGO guidelines and chronic kidney disease (CKD) staging. CKD was defined as abnormalities in kidney structure or function for ≥ three months with implications on health and meeting criteria for decreased GFR (<60 mL/min/1.73 m^2, stage G3a or greater).

Safety was not assessed for this subpopulation but was described by Anderson et al. for the parent phase IIb study population [22].

2.4. Oxidative damage endpoints

Oxidative damage endpoints were assessed in serum samples using a slot blotting technique and were assayed for protein carbonyls, 4HNE (4-Hydroxynonenal)-modified proteins, and 3-Nitrotyrosine (3NT) (Fig. 5) using the methods described below:

Immuno-slot-blotting for 4HNE-modified proteins and* 3-NT *adducted proteins: Plasma samples were diluted in 10 mM Diethylenetriaminepentaacetic acid (DETAPAC)/PBS/Roche Mini Protease inhibitor buffer (Sigma, # 11836153001). Protein concentration was measured using the Pierce BCA Protein Assay (Thermo, #23227). A series of positive controls were made for 3-NT by spiking 2 mg/mL transferrin with 100–0.001 μM peroxynitrite (Cayman, #81565)

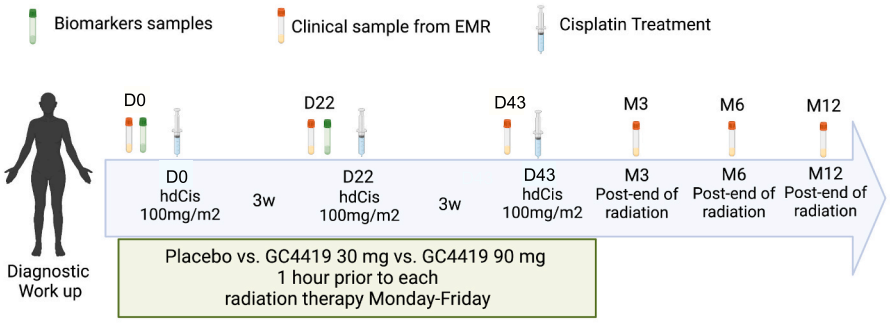

Illustration 1. Treatment Timeline and sample collection.

followed by incubation in at 37 °C for 30 min 5 μg of protein from sample and standards were used for 3-NT detection. Protein was loaded into Hoefer PR648 slot blot manifold (Hoefer, #PR648) after assembly according to the manufacturer's instruction. For 3-NT, following sample exposure to the membrane under vacuum pressure, the membrane was blocked in 5% milk/TBST for 1 h at room temperature. Following a wash cycle, the membrane was incubated with rabbit anti – 3-NT [1:200] (Cayman, #1019950) in 5% milk/TBST, overnight at 4 °C. After another wash cycle, the membrane was incubated with Anti-Rabbit IgG – peroxidase [1:10,000] (Sigma, #A6154) for 1 h at room temperature. After incubation, the membrane was put through another wash cycle and then incubated in Pierce ECL 2 Western Blotting Substrate (Thermo Scientific, # 80196) for 5 min and developed by x-ray film. Densitometry was done using ImageJ and results were normalized to total protein using Ponceau S staining (0.5% Ponceau S/0.1% Acetic Acid) (Fisher Scientific, #BP103-10).

4-HNE-modified protein positive controls were made as previously described [24] by spiking 2 mg/mL bovine serum albumin (BSA) with 100–0.001 μM 4-hydroxynonenal (Cayman, #32100) followed by incubation in at 37 °C for 30 min. Ten ug protein were utilized for 4-HNE--modified protein detection. After removal of the membrane from the apparatus and drying followed by reactivation with methanol for 1 min, and incubation in 80% 100 mM 3-(N-morpholino) propanesulfonic acid (MOPS)/20% methanol for 5 min, the membrane was incubated in 250 mM sodium borohydride (Aldrich, # 480886) at room temperature for 15 min to stabilize Schiff bases and Michael adducts. The membrane was then washed three times in dIH_2O and once in PBS before the membrane was blocked in 5% milk/TBST for 1 h at room temperature. Following wash cycle with TBST, the membrane was incubated with rabbit anti – 4HNE [1:2000] (Millipore, #ABN249) in 5% milk/TBST overnight at 4 °C. The membrane was then incubated with Anti-Rabbit IgG – peroxidase [1:10,000] (Sigma, #A6154) for 1 h at room temperature after another wash cycle. Following another wash cycle, the membrane was incubated in Pierce ECL 2 Western Blotting Substrate (Thermo Scientific, # 80196) for 5 min and visualized by x-ray film. Densitometry was done on ImageJ using the area under the curve after subtracting the background. Results were normalized to total protein using Ponceau S staining (0.5% Ponceau S/0.1% Acetic Acid) (Fisher Scientific, #BP103-10).

Detection of Carbonylated Proteins by Dinitrophenylhydrazine Derivatization: Plasma was collected from whole blood using a Heparin anticoagulant followed by centrifugation at 1000×*g* for 10 min at 4 °C. Protein Carbonyls were detected utilizing a Protein Carbonyl Colorimetric Assay Kit (Cayman, #10005020). Briefly, protein samples are derivatized by making use of the reaction between 2,4-dinitrophenylhydrazine and protein carbonyls. The formation of a Schiff base produces the corresponding hydrazone which can be analyzed spectrophotometrically at 360–385 nm. Results are normalized to the total protein used per well.

2.5. Iron panel analysis

Laboratory tests for iron panels were assessed in serum samples thawed on ice and stored at 4 °C overnight before analysis. Ferritin (Fe-blood), Iron saturation (Fe-Saturation), Transferrin (TfR), and Total Iron binding capacity (TIBC) levels were evaluated by the University of Iowa Diagnostic Laboratories using an electrochemiluminescence immunoassay (Cobas 7558 by Roche) that is used for standard clinical diagnostic protocols.

2.6. Statistical methods

Fisher's exact tests were used to compare categorical variables, and t-tests were used to compare continuous variables between treatment groups. Changes in renal laboratory values (eGFR, creatinine, BUN) were calculated from baseline to each subsequent assessment time point [(pre-hdCis-RT (**D0**), 3 weeks (**D22**), 6 weeks (**D43**), and 3 months (**M3**), 6 months (**M6)** and 12 months (**M12**) post-RT]. Mean estimates and 95% confidence intervals for changes from baseline in renal function were estimated using linear mixed effects regression models to account for the longitudinally correlated nature of repeated assessments at unequal time spacing between visits with a spatial power correlation structure. Repeated measures ANOVAs were used to evaluate mean changes in renal metrics, functional renal biomarkers, and iron metabolic proteins from D0 to D22 between treatment groups. All statistical testing was two-sided and assessed for significance at the 5% level using SAS v9.4 (SAS Institute, Cary, NC).

3. Results

The parent phase IIb trial (GT-201; NCT02508389) involved 44 US and Canadian sites that enrolled 223 patients, 217 of whom received at least one infusion of AVA, or placebo as described previously [22]. The overall goal of the parent trial was to compare the efficacy and safety of AVA to reduce the duration, incidence, and severity of severe oral mucositis (SOM). Among patients included in this study, baseline characteristics were comparable across the three treatment groups (Placebo, and 30 mg and 90 mg AVA) (Table 1) with at least seven patients from each group assessed for changes in renal function and biomarkers of renal injury (Illustration 1). Since the current report was an exploratory and retrospective analysis, only a small subset of subjects participating in the phase IIB study agreed to have additional analysis to assess renal function (Table 1). To assess longitudinal changes in renal function by treatment cohort, we followed markers of renal function (serum BUN and creatinine) and calculated estimated GFR (eGFR) (Fig. 1). The trends seen for each group are generally reflected in those for the individuals in that group (Fig. 2A and B).

Beginning as early as **D43**, a trend to less reduction in group mean eGFR is seen with 90 mg AVA (Fig. 1A). By three months completion of radiation (**M3**), a mean eGFR reduction from pre-hdCIS-RT (**D0)** of 22.8 ml/min/1.73 m^2 in the placebo-treated group contrasts with a 6.9 ml/min/1.73 m^2 reduction in the 90 mg AVA group, which is a clinically and statistically significant improvement ($p = 0.02$) (Fig. 1A). Similarly, creatinine levels were also significantly different between the 90 mg AVA and the placebo groups ($p = 0.02$), consistent with a trend in serum BUN (Fig. 1B). No difference was observed in eGFR at **M3** between placebo and 30 mg AVA groups (Fig. 1A), though numerically 30 mg may have lessened the increase in BUN (Fig. 1C). Collectively, these data suggest that 90 mg AVA may be effective at protecting against renal dysfunction in the first 3 months post therapy, while 30 mg AVA has a lesser effect, if at all.

A significant difference in eGFR was also observed at **M6** between the placebo and 90 mg AVA groups (mean eGFR decline from baseline (**D0**) of 24.7 ml/min/1.73 m^2 *vs.* 8.3 ml/min/1.73 m^2; $p = 0.04$) (Fig. 1A). Interestingly, this attenuation of mean eGFR decline was even more pronounced at **M12** (33.0 ml/min/1.73 m^2 placebo vs. 5.0 ml/min/1.73 m^2 90 mg AVA; p = 0–01) (Fig. 1A). Similarly, **M12** creatinine levels also significantly favored the 90 mg AVA group over placebo ($p = 0.02$), consistent with a trend in serum BUN (Fig. 1C). In fact, comparing mean eGFR loss longitudinally across **M3** through **M12**, it appears that 90 mg AVA maintains renal function over this period, while the placebo group shows progressive decline (Fig. 1A). Again, no difference was observed in eGFR at **M6** between placebo and 30 mg AVA groups (Fig. 1A), though the trend to 30 mg lessening the increase in BUN remained (Fig. 1C). By **M12**, however, there are numerical trends favoring 30 mg AVA compared to placebo in all three metrics (Fig. 1). Together, these data suggest that 90 mg AVAcan also help reduce, or even possibly prevent further, loss of renal function due to cisplatin in the CKD phase, while 30 mg AVA may offer dose-dependent support of this benefit.

Overall, these changes in renal functional markers, are clinically significant and relevant for screening, diagnosis, and monitoring kidney injury progression following hdCis-RT. Although the analysis is based on

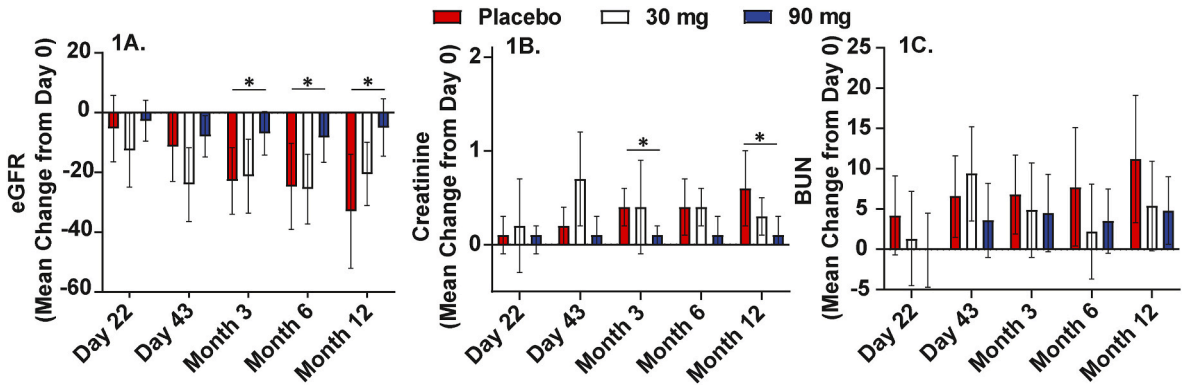

Fig. 1. Mean changes in renal metrics up to one year following hdCis-RT. Mean change in eGFR **(1A.)**, Creatinine **(1B.)**, and BUN **(1C.)** from pre-hdCis-RT (**D0**) and p-values for the comparison between treatment groups at noted time points (* = $p < 0.05$). Highlighted values indicate a statistically significant difference in mean change from **D0** between treatment groups. Changes in renal metrics (eGFR, Creatinine, BUN) were calculated from **D0** to each subsequent assessment time point (Day 22, Day 43, Month 3, Month 6, Month 12). Linear mixed-effects regression models were used to evaluate changes over time between treatment groups using SAS v9.4 (SAS Institute, Cary, NC). Random effects were included to account for the longitudinally correlated nature of repeated assessments at unequal time spacing between visits with a spatial power correlation structure.

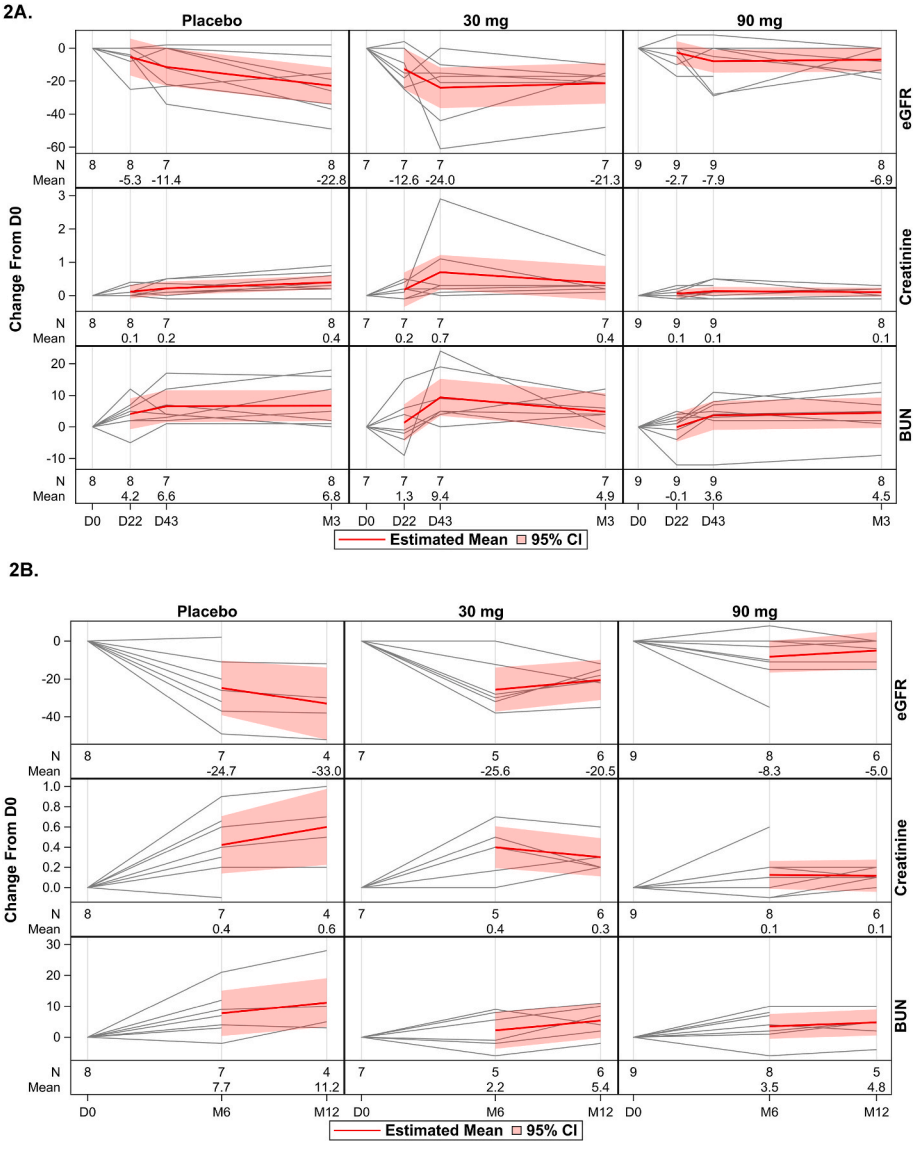

Fig. 2. Changes in renal metrics in AKD and CKD phase of renal injury. (2A). Estimated glomerular Filtration Rate (eGFR), Creatinine, and Blood Urea Nitrogen (BUN) levels were evaluated pre-hdCis-RT (**D0**), 3 weeks (**D22**), and 6 weeks (**D43**), and 3 months (**M3**) post-RT. The gray lines indicate each individual patient's trajectory whereas, the red line indicates the estimated mean along with the 95% confidence interval (CI). **(2B).** Estimated glomerular Filtration Rate (eGFR), Creatinine, and Blood Urea Nitrogen (BUN) levels were evaluated pre-hdCis-RT (**D0**), 6 months (**M6**), and 12 months (**M12**) post-RT. The gray lines indicate each individual patient's trajectory whereas, the red line indicates the estimated mean along with the 95% confidence interval (CI). Changes in renal metrics (BUN, creatinine, eGFR) were calculated from **D0** to each subsequent assessment time point (Day 22, Day 43, Month 3, Month 6, Month 12). Linear mixed-effects regression models were used to evaluate changes over time between treatment groups using SAS v9.4 (SAS Institute, Cary, NC). Random effects were included to account for the longitudinally correlated nature of repeated assessments at unequal time spacing between visits with a spatial power correlation structure. (For interpretation of the references to colour in this figure legend, the reader is referred to the Web version of this article.)

a small subset of subjects, these striking and clinically meaningful improvements with 90 mg AVA will be interrogated as prospectively defined exploratory endpoints in long-term follow-up of roughly 400 subjects. These subjects participated in the ROMAN Phase 3 trial of avasopasem manganese for SOM (NCT03689712).

To assess additional markers involved in renal dysfunction that could predict response to nephroprotective therapy and CKD progression, we measured biomarkers of tubulointerstitial disease in serum samples pre-hdCis-RT (**D0**) and at three weeks (**D22**) for patients treated in the placebo and 90 mg AVA groups. The **D22** biomarker levels were measured 3 weeks after the initial cisplatin treatment, just prior to the second cisplatin dose. No statistically significant baseline differences were noted between treatment groups. Results indicate a statistically significant difference in the average change in serum levels of Epithelial Growth Factor (EGF) between treatment groups ($p < 0.01$), with the 90 mg AVA treatment group demonstrating increased EGF whereas the placebo group saw a decline in EGF. (Fig. 3A). EGF is known to stimulate proximal tubule cell proliferation [25-27], and is indicative of a potential increase in renal reserve and recovery from hdCis-RT treatment. Tumor necrosis factor alpha (TNFα), an inflammatory cytokine that correlates with the progression of kidney disease [28,29], and is a mediator of inflammation whereas, the expression of TNFR2 is mainly restricted to immune and endothelial cells [30,31] While not statistically significant, our results indicate treatment with 90 mg AVA resulted

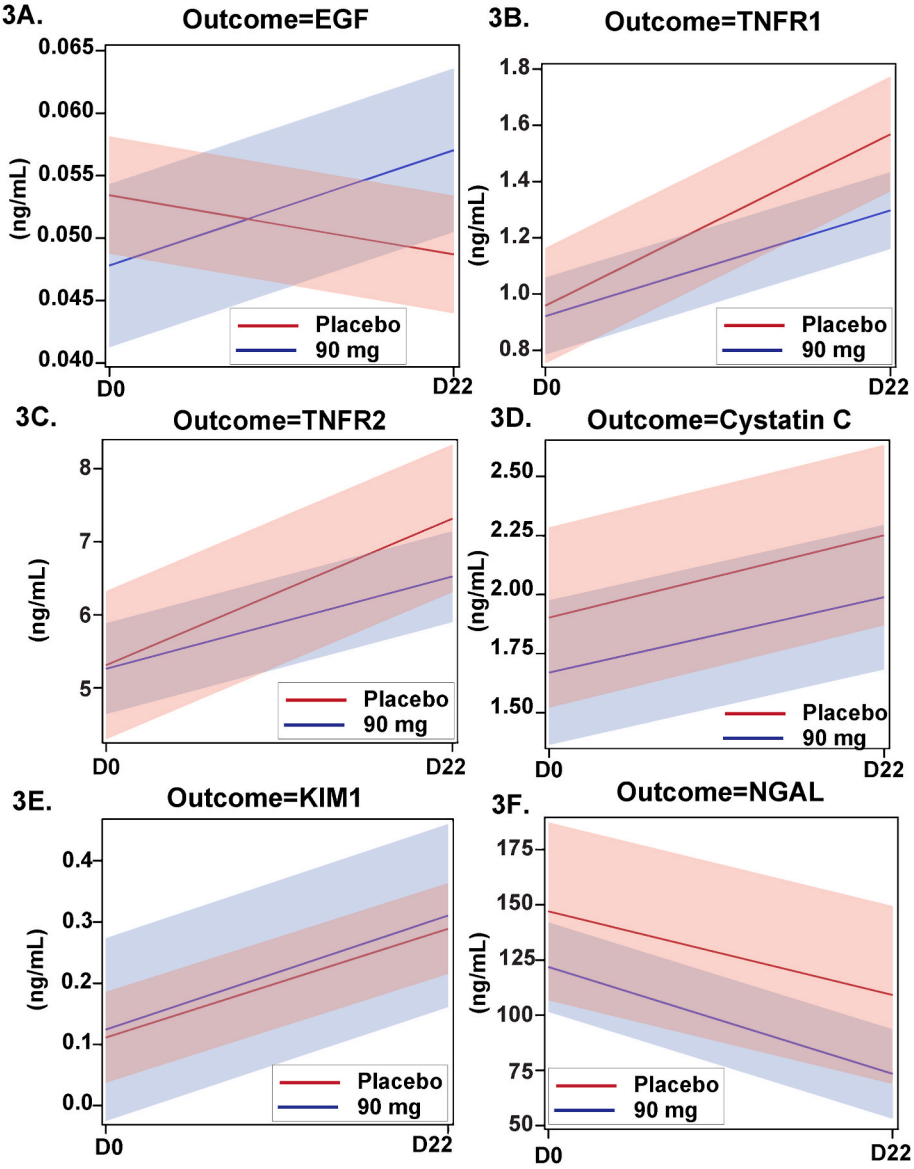

3G. Baseline Differences

Outcome	P - value
NGAL	0.27
EGF	0.17
TNFR1	0.76
TNFR2	0.93
Cystatin C	0.35
KIM1	0.88

3H. Slope Differences

Outcome	P-value
NGAL	0.49
EGF	**<.01***
TNFR1	0.11
TNFR2	0.26
Cystatin C	0.90
KIM1	0.93

Fig. 3. Expression of functional renal biomarkers in patients treated with placebo and 90 mg AVA serum samples. (**3A.**) Mean changes in Epidermal Growth Factor (EGF expression in Placebo *vs.* 90 mg AVA at D0 and D22. Mean changes in levels of kidney biomarkers using an MSD sandwich immunoassay with U-PLEX platform from Mesoscale including (**3B.**) Tumor Necrosis Factor Receptor 1 (TNFR1), (**3C.**) Tumor Necrosis Factor Receptor 2 (TNFR2), (**3D.**) Cystatin C, and (**3E.**) Kidney Injury Molecule 1 (KIM1) and (**3F.**) Neutrophil Gelatinase-Associated Lipocalin (NGAL). Although no baseline differences were observed in the different biomarkers (**3G.**), the mean changes in EGF levels (**3A.**) between the placebo *vs.* 90 mg AVA-treated group were significantly different with a p-value of <0.01 (**3H.**). Repeated measures ANOVAs were used to evaluate mean changes from **D0** to **D22** between treatment groups using SAS v9.4 (SAS Institute, Cary, NC).

in a smaller increase in TNFR1 (Fig. 3B) and TNFR2 (Fig. 3C), on average, compared to placebo, indicative of a potential reduction in the tubulointerstitial inflammation post-hdCis treatment. No significant treatment group differences were observed in the serum levels of Cystatin C (Fig. 3D) and Kidney Injury Molecule-1 (KIM-1) (Fig. 3E) and NGAL (Fig. 3F) between **D0** and **D22** (3 weeks after cisplatin exposure). The serum cystatin C, a kidney function marker, is consistent with our serum creatinine data and was not statistically significant amongst treatment groups between **D0** and **D22** (Fig. 1B). Analysis of other biomarkers of tubulointerstitial disease including osteoactivin (Fig. 4A), osteopontin (Fig. 4B), and uromodulin (Fig. 4C) did not show any significant treatment group differences between D0 and D22. Although the levels of tubulointerstitial injury were measured in the renal recovery phase after a single cisplatin treatment, our results suggest that selected biomarkers of tubulointerstitial disease could be utilized for early identification of patients at risk of CKD progression following cisplatin treatment and could potentially be utilized for early identification of nephroprotective therapy response.

Our group has previously shown that cisplatin treatment alters mitochondrial metabolism, resulting in mitochondrially derived reactive oxygen species (ROS) [12,13]. Towards this end, oxidative damage endpoints were assessed in serum samples using protein carbonyls (Fig. 5A and B), and 3-Nitrotyrosine (3NT) (Fig. 5C–E), and 4HNE-modified proteins (Fig. 5F–H). Results indicate no significant changes in oxidative damage markers in the AKD phase of renal injury.

Since redox-active iron is a critical regulator of ROS damage with the iron-binding protein, ferritin, responsible for preserving cellular iron homeostasis, samples were also analyzed for systemic changes in iron homeostasis. We assessed levels of iron-related circulating markers including Transferrin (Tf), Total Iron Binding Capacity (TIBC), total iron (Fe-blood), iron saturation (Fe-saturation), and Ferritin. No different temporal patterns were observed regarding circulating Tf or TIBC (Fig. 6A and B). While no significant differences were observed between placebo and 90 mg AVA-treated patients (potentially due to the limited sample size), significant increases were observed in total iron (Fe-blood) (Fig. 6C), Fe-saturation (Fig. 6D) and Ferritin (Fig. 6E) between baseline **D0** and **D22** in patients receiving 90 mg AVA. Differences in Fe-Saturation (Fig. 6D) and Ferritin (Fig. 6E) were also observed in placebo-treated patients between baseline **D0** and **D22**. Ferritin can function as a marker of acute and chronic inflammatory responses along with iron deficiency [30-32], but no significant differences were observed in subjects receiving 90 mg AVA *vs.* the placebo group (Fig. 6F)..

4. Discussion

Renal insufficiency is a frequent morbidity following treatment with high-dose cisplatin that can seriously impact cancer patient survivorship. Assessment of early and longitudinal changes in renal biomarkers may aid in identifying patients at risk of CKD and the development of nephroprotective therapies. Oxidative stress plays a significant role in the pathogenesis of cisplatin-induced nephrotoxicity with excess ROS overwhelming the defensive systems in kidney tubules resulting in epithelial cell damage and fibrosis [3]. Furthermore, these increased levels of ROS are also associated with the transition of AKI to AKD to CKD [6,33]. Recent preclinical data suggest that a persistent increase in mitochondrial superoxide mediates CKD, and that avasopasem manganese (AVA) protects against cisplatin-induced kidney injury [12,13].

Cisplatin-induced CKD is a significant health concern; however, the progression of renal disease is slow to manifest with distinct symptoms

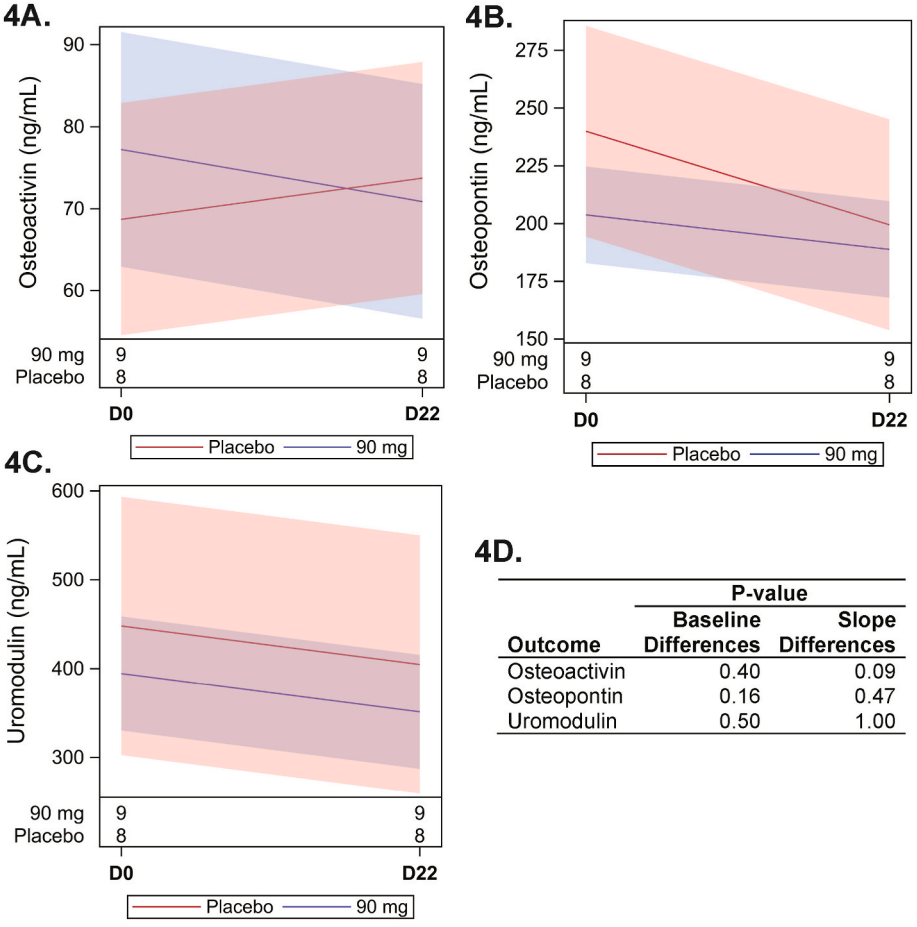

4D.

	P-value	
Outcome	Baseline Differences	Slope Differences
Osteoactivin	0.40	0.09
Osteopontin	0.16	0.47
Uromodulin	0.50	1.00

Fig. 4. Expression of functional renal biomarkers in patients treated with placebo and 90 mg AVA serum samples. Changes in levels of kidney biomarkers using an MSD sandwich immunoassay with U-PLEX platform from Mesoscale including (**4A.**) Osteoactivin, (**4B.**) Osteopontin, and (**4C.**) Uromodulin. No statistically significant differences were observed (**4D.**). Repeated measures ANOVAs were used to evaluate mean changes from D0 to D22 between treatment groups using SAS v9.4 (SAS Institute, Cary, NC).

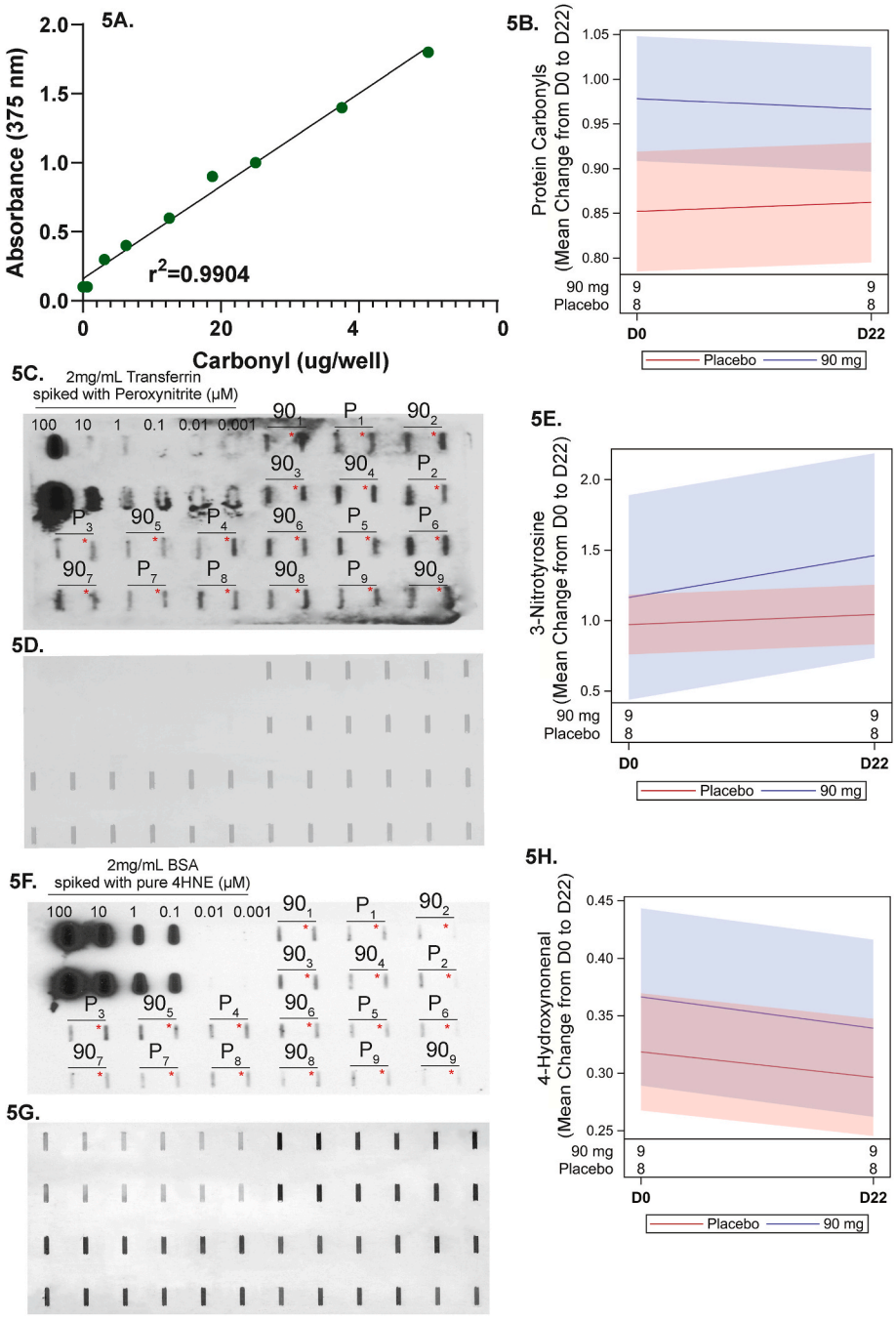

Fig. 5. Changes in oxidative damage endpoints. Oxidative markers were assessed in serum samples using a dot blot and were assayed for protein carbonyls (**5A. and 5B.**), 4HNE modified proteins (4-Hydroxynonenal) (**5C-5E.**), and 3-Nitrotyrosine (3NT) (**5F–5H.**). Standard curves were generated for each of the three damage endpoints using increasing concentrations of Carbonyl (**5A.**), 2 mg/mL Transferrin spiked with increasing concentrations of Peroxynitrite (**5C.**), and 2 mg/mL Transferrin spiked with increasing concentrations of pure 4-HNE (**5F.**). (P_1 – P_9) denotes the placebo-treated patients whereas, (90_1- 90_9) denotes 90 mg AVA-treated patient serums in panels (**5C.**) and (**5F.**). Each patient sample has a set of two bands with the first band representing the sample from D_0 and the second band representing the sample collected on D_{22} (**5C.** and **5F.**). Blots for 3-Nitrotyrosine and 4-HNE were stained with Ponceau as a protein loading control (**5D.**) and (**5G.**) respectively. Quantification for 3-Nitrotyrosine and 4-HNE normalized to the protein is depicted in panels (**5E.**) and (**5H.**) respectively. Repeated measures ANOVAs were used to evaluate mean changes from D0 to D22 between treatment groups using SAS v9.4 (SAS Institute, Cary, NC).

presenting years after completion of therapy. As such, changes in tubulointerstitial biomarkers early in the disease process, i.e., in the first 3–12 months following cisplatin exposure, may provide prognostic value to predict chronic kidney outcomes. Currently a considerable decline in eGFR is a surrogate measure of kidney health that can be assessed over time. In this retrospective analysis of phase IIb subjects' clinical lab data and serum samples, 90 mg AVA showed significant renal function improvement following hdCis-RT as reflected by the minimal decreases in eGFR seen in the 90 mg AVA group. The protective effect in eGFR first manifested by at least three months post-therapy and was more evident one year (**M12**) after completion of cisplatin therapy. In the first 3 months (**D0** *vs.* **M3**), placebo-treated subjects had a greater mean decline in eGFR (22.8 ml/min/1.73 m^2) compared to 90 mg AVA subjects (6.9 ml/min/1.73 m^2). This clinically relevant difference may be predictive of progression to kidney disease and thus have significant prognostic implications on the patient's quality of life. Moreover, minimal further decrease in eGFR was evident at one year for the 90 mg AVA-treated subjects (5 ml/min/1.73 m^2 decline **D0** *vs.* **M12**) while the placebo subjects continued to deteriorate (33 ml/min/1.73 m^2 decline) indicative of renal function preservation and potential prevention of CKD onset and/or progression.

4.1. *Changes in biomarkers and kidney function*

As this retrospective analysis was focused solely on renal function and biomarkers of kidney damage, no data beyond this was collected on the safety and tolerability of either avasopasem or the underlying radiation and cisplatin regimens. In the parent GT-201 trial itself, avasopasem appeared well-tolerated, with an adverse event profile similar to that seen in the placebo group.

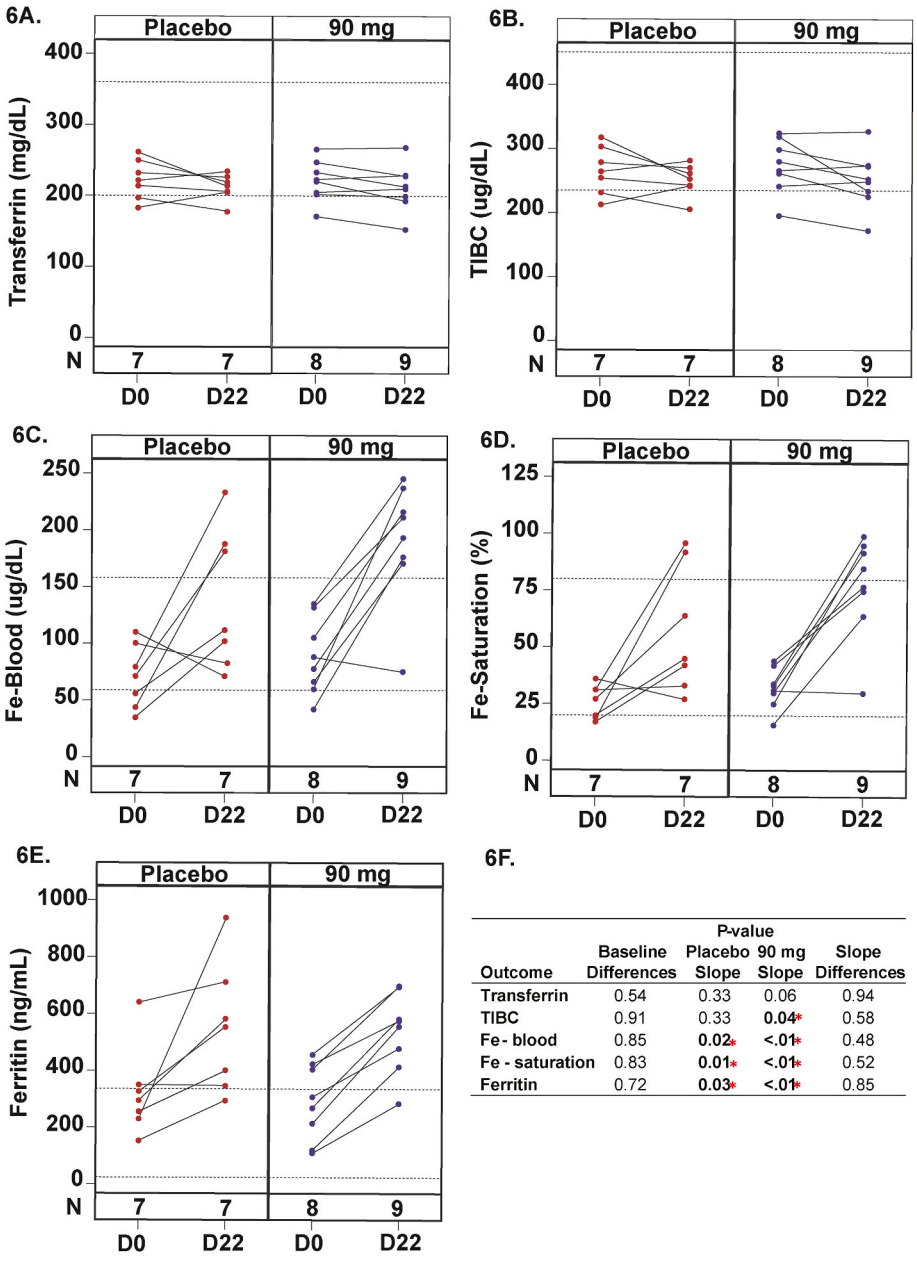

6F.

Outcome	Baseline Differences	P-value Placebo Slope	P-value 90 mg Slope	Slope Differences
Transferrin	0.54	0.33	0.06	0.94
TIBC	0.91	0.33	**0.04***	0.58
Fe - blood	0.85	**0.02***	**<.01***	0.48
Fe - saturation	0.83	**0.01***	**<.01***	0.52
Ferritin	0.72	**0.03***	**<.01***	0.85

Fig. 6. Analysis of changes in proteins involved in iron metabolism in placebo *vs.* 90 mg AVA treated groups. Systemic changes in iron homeostasis were assessed by analyzing changes in levels of iron metabolic proteins including (**6A.**) Serum Transferrin, (**6B.**) Total Iron Binding Capacity (TIBC), (**6C.**) Total iron (Fe-Blood), (**6D.**) Iron Saturation levels (Fe-Saturation), and (**6E.**) Ferritin. No statistically significant differences between treatment groups were noted, but some statistically significant mean changes were noted within treatment groups (*$p < 0.05$) (**6F.**). Repeated measures ANOVAs were used to evaluate mean changes from D0 to D22 between treatment groups using SAS v9.4 (SAS Institute, Cary, NC).

In the recent past, several studies have elucidated a direct correlation between the rate of decline in kidney function and the changes in renal tubule-interstitial biomarkers levels [34-36]. Numerous tubular proteins, including NGAL, Cystatin C, EGF, TNFR1, TNFR2, and KIM-1 are reliable biomarkers of acute and chronic renal injury. The EGF family of mitogenic proteins plays a role in normal cell growth and differentiation, renal physiology, and tissue repair. Its increased expression indicates a regenerative mechanism making it a critical biomarker of renal repair [37,38]. Significantly increased levels of EGF three weeks after initial cisplatin treatment (**D22**) in the 90 mg AVA-treated group compared to the placebo suggest an enhanced renal function reserve following cisplatin exposure either by protecting from cisplatin nephrotoxicity or by promoting renal repair.

4.2. Iron metabolism and CKD

The intriguing results observed regarding circulating iron suggest a potential iron metabolic shift may be occurring in patients treated with AVA. While no changes in Tf or TIBC were observed on D22, the increased magnitude of iron and iron saturation suggests that 90 mg AVA may support intestinal iron uptake from dietary sources and is independent of GFR changes. Iron deficiency anemia is a common side effect of CKD as 17–50% of patients with stage 3–5 CKD can become iron deficient [39]. The onset of true iron deficiency may be due to enhanced liver hepcidin production, ultimately resulting in decreased ferroportin–mediated iron uptake through enterocytes [40]. In addition, patients with CKD appear to have significant iron accumulation in the proximal tubule associated with increased expression of iron import proteins, iron storage (ferritin heavy/light chains), and decreased iron export (ferroportin) compared to healthy controls [41]. Thus, the shift towards enriched circulating iron we observed supports a hypothesis that AVA is protective against $O_2^{\bullet-}$-mediated detrimental tissue iron accumulation while simultaneously mitigating inflammation-induced hepcidin production allowing for the maintenance of higher levels of circulating iron. While this hypothesis is based on preliminary clinical observations and may be largely speculative, it remains easily testable

and warrants further investigation in preclinical and biochemical model systems.

5. Summary

Overall, this study is a novel post-hoc exploratory analysis of kidney injury markers during cisplatin therapy and renal function through one-year post-treatment in a phase IIb clinical trial designed to evaluate the amelioration of RT-associated severe oral mucositis. Limitations acknowledged in this study include the small number of patient samples, the limited available data to assess renal endpoints, and its retrospective nature; however, this study is strengthened by the significant changes in eGFR following cisplatin exposure in both in the AKD and CKD phases of renal injury. Despite the lack of acute change in serum creatinine in our cohort, our findings in the placebo group are aligned with known permanent reduction in eGFR in cisplatin treated patients that is more recognizable about four months and up to one year following cisplatin treatment [4,8,42]. This study supports a hypothesis that a selective dismutase mimetic could offer potential for kidney protection following hdCis. The results reported here are hypothesis-generating for further clinical study and supported the prospective exploratory assessment of CKD in a subsequent randomized, placebo-controlled, double-blind trial of avasopasem manganese in SOM (NCT03689712), full results of which are pending publication.

Declaration of competing interest

Drs. Spitz and Allen acknowledge support for their laboratory efforts from a sponsored research agreement from Galera Therapeutics, Inc. Dr. Beardsley is an employee of and owns stock in, Galera Therapeutics, Inc. Dr. Holmlund owns stock in Galera Therapeutics, Inc. No potential conflicts of interest were disclosed by the other authors.

Data availability

Data will be made available on request.

Acknowledgments

The authors would like the acknowledge Gareth Smith for assistance with graphics and Ann Tomanek-Chalkley for technical assistance. These studies were supported by a sponsored research agreement with Galera Therapeutics, Inc and NIH T32 CA078586 and P01 CA217797. Galera sponsored/provided funding for the underlying Phase 2b from which the patients retrospectively assessed in the present analysis were drawn.

Appendix A. Supplementary data

Supplementary data to this article can be found online at https://doi.org/10.1016/j.redox.2022.102599.

References

[1] S.F. Oosting, R.I. Haddad, Best Practice in systemic therapy for head and neck squamous cell carcinoma, Front. Oncol. 9 (2019) 815.
[2] M. van der Vorst, E.C.W. Neefjes, E.C. Toffoli, J.E.W. Oosterling-Jansen, M. R. Vergeer, C.R. Leemans, M.P. Kooistra, J. Voortman, H.M.W. Verheul, Incidence and risk factors for acute kidney injury in head and neck cancer patients treated with concurrent chemoradiation with high-dose cisplatin, BMC Cancer 19 (2019) 1066.
[3] R.P. Miller, R.K. Tadagavadi, G. Ramesh, W.B. Reeves, Mechanisms of cisplatin nephrotoxicity, Toxins 2 (2010) 2490–2518.
[4] S. Latcha, E.A. Jaimes, S. Patil, I.G. Glezerman, S. Mehta, C.D. Flombaum, Long-term renal outcomes after cisplatin treatment, Clin. J. Am. Soc. Nephrol. 11 (2016) 1173–1179.
[5] L.S. Chawla, R. Bellomo, A. Bihorac, S.L. Goldstein, E.D. Siew, S.M. Bagshaw, D. Bittleman, D. Cruz, Z. Endre, R.L. Fitzgerald, L. Forni, S.L. Kane-Gill, E. Hoste, J. Koyner, K.D. Liu, E. Macedo, R. Mehta, P. Murray, M. Nadim, M. Ostermann, P. M. Palevsky, N. Pannu, M. Rosner, R. Wald, A. Zarbock, C. Ronco, J.A. Kellum, W. Acute Disease Quality Initiative, Acute kidney disease and renal recovery: consensus report of the Acute Disease Quality Initiative (ADQI) 16 Workgroup, Nat. Rev. Nephrol. 13 (2017) 241–257.
[6] L.S. Chawla, P.W. Eggers, R.A. Star, P.L. Kimmel, Acute kidney injury and chronic kidney disease as interconnected syndromes, N. Engl. J. Med. 371 (2014) 58–66.
[7] K.R. McMahon, S.R. Rassekh, K.R. Schultz, T. Blydt-Hansen, G.D.E. Cuvelier, C. Mammen, M. Pinsk, B.C. Carleton, R.T. Tsuyuki, C.J.D. Ross, A. Palijan, L. Huynh, M. Yordanova, F. Crepeau-Hubert, S. Wang, D. Boyko, M. Zappitelli, Applying Biomarkers to Minimize Long-Term Effects of Childhood/Adolescent Cancer Treatment Research Study, G, Epidemiologic characteristics of acute kidney injury during cisplatin infusions in children treated for cancer, JAMA Netw. Open 3 (2020), e203639.
[8] M. Zappitelli, J.H. Greenberg, S.G. Coca, C.D. Krawczeski, S. Li, H.R. Thiessen-Philbrook, M.R. Bennett, P. Devarajan, C.R. Parikh, Translational Research Investigating Biomarker Endpoints in Acute Kidney Injury, C, Association of definition of acute kidney injury by cystatin C rise with biomarkers and clinical outcomes in children undergoing cardiac surgery, JAMA Pediatr. 169 (2015) 583–591.
[9] M. Ostermann, A. Zarbock, S. Goldstein, K. Kashani, E. Macedo, R. Murugan, M. Bell, L. Forni, L. Guzzi, M. Joannidis, S.L. Kane-Gill, M. Legrand, R. Mehta, P. T. Murray, P. Pickkers, M. Plebani, J. Prowle, Z. Ricci, T. Rimmele, M. Rosner, A. D. Shaw, J.A. Kellum, C. Ronco, Recommendations on acute kidney injury biomarkers from the acute disease quality initiative consensus conference: a consensus statement, JAMA Netw. Open 3 (2020), e2019209.
[10] K.R. McMahon, S. Rod Rassekh, K.R. Schultz, M. Pinsk, T. Blydt-Hansen, C. Mammen, R.T. Tsuyuki, P. Devarajan, G.D. Cuvelier, L.G. Mitchell, S. Baruchel, A. Palijan, B.C. Carleton, C.J. Ross, M. Zappitelli, Applying Biomarkers to Minimize Long-Term Effects of Childhood/Adolescent Cancer Treatment Research, G, Design and methods of the pan-Canadian applying biomarkers to minimize long-term effects of childhood/adolescent cancer treatment (ABLE) nephrotoxicity study: a prospective observational cohort study, Can J Kidney Health Dis 4 (2017), 2054358117690338.
[11] Z.Y. Bhat, P. Cadnapaphornchai, K. Ginsburg, M. Sivagnanam, S. Chopra, C. K. Treadway, H.S. Lin, G. Yoo, A. Sukari, M.D. Doshi, Understanding the risk factors and long-term consequences of cisplatin-associated acute kidney injury: an observational cohort study, PLoS One 10 (2015), e0142225.
[12] K.A. Mapuskar, H. Wen, D.G. Holanda, P. Rastogi, E. Steinbach, R. Han, M. C. Coleman, M. Attanasio, D.P. Riley, D.R. Spitz, B.G. Allen, D. Zepeda-Orozco, Persistent increase in mitochondrial superoxide mediates cisplatin-induced chronic kidney disease, Redox Biol. 20 (2019) 98–106.
[13] K.A. Mapuskar, E.J. Steinbach, A. Zaher, D.P. Riley, R.A. Beardsley, J.L. Keene, J. T. Holmlund, C.M. Anderson, D. Zepeda-Orozco, J.M. Buatti, D.R. Spitz, B.G. Allen, Mitochondrial superoxide dismutase in cisplatin-induced kidney injury, Antioxidants 10 (2021).
[14] B.B. Ratliff, W. Abdulmahdi, R. Pawar, M.S. Wolin, Oxidant mechanisms in renal injury and disease, Antioxidants Redox Signal. 25 (2016) 119–146.
[15] N. Choi, R. Whitlock, J. Klassen, M. Zappitelli, R.C. Arora, C. Rigatto, J. Ho, Early intraoperative iron-binding proteins are associated with acute kidney injury after cardiac surgery, J. Thorac. Cardiovasc. Surg. 157 (2019) 287–297, e282.
[16] Z.M. Dimitrijevic, S.S. Salinger-Martinovic, R.J. Jankovic, B.P. Mitic, Elevated serum ferritin levels are predictive of renal function recovery among patients with acute kidney injury, Tohoku J. Exp. Med. 248 (2019) 63–71.
[17] S. Recalcati, P. Invernizzi, P. Arosio, G. Cairo, New functions for an iron storage protein: the role of ferritin in immunity and autoimmunity, J. Autoimmun. 30 (2008) 84–89.
[18] M.A. Knovich, J.A. Storey, L.G. Coffman, S.V. Torti, F.M. Torti, Ferritin for the clinician, Blood Rev. 23 (2009) 95–104.
[19] J.H. Lee, H. Jang, E.J. Cho, H.D. Youn, Ferritin binds and activates p53 under oxidative stress, Biochem. Biophys. Res. Commun. 389 (2009) 399–404.
[20] C.D. Heer, A.B. Davis, D.B. Riffe, B.A. Wagner, K.C. Falls, B.G. Allen, G.R. Buettner, R.A. Beardsley, D.P. Riley, D.R. Spitz, Superoxide dismutase mimetic GC4419 Enhances the oxidation of pharmacological ascorbate and its anticancer effects in an H(2)O(2)-dependent manner, Antioxidants 7 (2018).
[21] K.A. Mapuskar, K.H. Flippo, J.D. Schoenfeld, D.P. Riley, S. Strack, T.A. Hejleh, M. Furqan, V. Monga, F.E. Domann, J.M. Buatti, P.C. Goswami, D.R. Spitz, B. G. Allen, Mitochondrial superoxide increases age-associated susceptibility of human dermal fibroblasts to radiation and chemotherapy, Cancer Res. 77 (2017) 5054–5067.
[22] C.M. Anderson, C.M. Lee, D.P. Saunders, A. Curtis, N. Dunlap, C. Nangia, A.S. Lee, S.M. Gordon, P. Kovoor, R. Arevalo-Araujo, V. Bar-Ad, A. Peddada, K. Colvett, D. Miller, A.K. Jain, J. Wheeler, D. Blakaj, M. Bonomi, S.S. Agarwala, M. Garg, F. Worden, J. Holmlund, J.M. Brill, M. Downs, S.T. Sonis, S. Katz, J.M. Buatti, Phase IIb, randomized, double-blind trial of GC4419 versus placebo to reduce severe oral mucositis due to concurrent radiotherapy and cisplatin for head and neck cancer, J. Clin. Oncol. 37 (2019) 3256–3265.
[23] A.S. Levey, L.A. Stevens, Estimating GFR using the CKD Epidemiology Collaboration (CKD-EPI) creatinine equation: more accurate GFR estimates, lower CKD prevalence estimates, and better risk predictions, Am. J. Kidney Dis. 55 (2010) 622–627.
[24] B.G. Allen, S.K. Bhatia, J.M. Buatti, K.E. Brandt, K.E. Lindholm, A.M. Button, L. I. Szweda, B.J. Smith, D.R. Spitz, M.A. Fath, Ketogenic diets enhance oxidative stress and radio-chemo-therapy responses in lung cancer xenografts, Clin. Cancer Res. 19 (2013) 3905–3913.
[25] P. Wee, Z. Wang, Epidermal growth factor receptor cell proliferation signaling pathways, Cancers 9 (2017).

[26] D. Zepeda-Orozco, H.M. Wen, B.A. Hamilton, N.S. Raikwar, C.P. Thomas, EGF regulation of proximal tubule cell proliferation and VEGF-A secretion, Phys. Rep. 5 (2017).
[27] J. Chen, J.K. Chen, R.C. Harris, Deletion of the epidermal growth factor receptor in renal proximal tubule epithelial cells delays recovery from acute kidney injury, Kidney Int. 82 (2012) 45–52.
[28] V.D. Ramseyer, J.L. Garvin, Tumor necrosis factor-alpha: regulation of renal function and blood pressure, Am. J. Physiol. Ren. Physiol. 304 (2013) F1231–F1242.
[29] E. Mehaffey, D.S.A. Majid, Tumor necrosis factor-alpha, kidney function, and hypertension, Am. J. Physiol. Ren. Physiol. 313 (2017) F1005–F1008.
[30] D.B. Kell, E. Pretorius, Serum ferritin is an important inflammatory disease marker, as it is mainly a leakage product from damaged cells, Metallomics 6 (2014) 748–773.
[31] K.F. Kernan, J.A. Carcillo, Hyperferritinemia and inflammation, Int. Immunol. 29 (2017) 401–409.
[32] W. Wang, M.A. Knovich, L.G. Coffman, F.M. Torti, S.V. Torti, Serum ferritin: past, present and future, Biochim. Biophys. Acta 1800 (2010) 760–769.
[33] N.H. Lameire, A. Levin, J.A. Kellum, M. Cheung, M. Jadoul, W.C. Winkelmayer, P. E. Stevens, P. Conference, Harmonizing acute and chronic kidney disease definition and classification: report of a kidney disease: improving global outcomes (KDIGO) consensus conference, Kidney Int. 100 (2021) 516–526.
[34] D. Bolignano, A. Lacquaniti, G. Coppolino, V. Donato, S. Campo, M.R. Fazio, G. Nicocia, M. Buemi, Neutrophil gelatinase-associated lipocalin (NGAL) and progression of chronic kidney disease, Clin. J. Am. Soc. Nephrol. 4 (2009) 337–344.
[35] A.O. Phillips, The role of renal proximal tubular cells in diabetic nephropathy, Curr. Diabetes Rep. 3 (2003) 491–496.
[36] A.A. Eddy, E.G. Neilson, Chronic kidney disease progression, J. Am. Soc. Nephrol. 17 (2006) 2964–2966.
[37] A. Staruschenko, O. Palygin, D.V. Ilatovskaya, T.S. Pavlov, Epidermal growth factors in the kidney and relationship to hypertension, Am. J. Physiol. Ren. Physiol. 305 (2013) F12–F20.
[38] L.R. Harskamp, R.T. Gansevoort, H. van Goor, E. Meijer, The epidermal growth factor receptor pathway in chronic kidney diseases, Nat. Rev. Nephrol. 12 (2016) 496–506.
[39] S. Stancu, A. Stanciu, A. Zugravu, L. Barsan, D. Dumitru, M. Lipan, G. Mircescu, Bone marrow iron, iron indices, and the response to intravenous iron in patients with non-dialysis-dependent CKD, Am. J. Kidney Dis. 55 (2010) 639–647.
[40] E.K. Batchelor, P. Kapitsinou, P.E. Pergola, C.P. Kovesdy, D.I. Jalal, Iron deficiency in chronic kidney disease: updates on pathophysiology, diagnosis, and treatment, J. Am. Soc. Nephrol. 31 (2020) 456–468.
[41] S. van Raaij, R. van Swelm, K. Bouman, M. Cliteur, M.C. van den Heuvel, J. Pertijs, D. Patel, P. Bass, H. van Goor, R. Unwin, S.K. Srai, D. Swinkels, Tubular iron deposition and iron handling proteins in human healthy kidney and chronic kidney disease, Sci. Rep. 8 (2018) 9353.
[42] K.R. McMahon, A. Lebel, S.R. Rassekh, K.R. Schultz, T.D. Blydt-Hansen, G.D. E. Cuvelier, C. Mammen, M. Pinsk, B.C. Carleton, R.T. Tsuyuki, C.J.D. Ross, L. Huynh, M. Yordanova, F. Crepeau-Hubert, S. Wang, A. Palijan, J. Lee, D. Boyko, M. Zappitelli, Applying Biomarkers to Minimize Long-Term Effects of Childhood/Adolescent Cancer Treatment Research Study, G, Acute kidney injury during cisplatin therapy and associations with kidney outcomes 2 to 6 months post-cisplatin in children: a multi-centre, prospective observational study, Pediatr. Nephrol. (2022).